Automatica 131 (2021) 109744

Contents lists available at ScienceDirect

Automatica

journal homepage: www.elsevier.com/locate/automatica

Brief paper

A behavioural dynamic model for constant power loads in single-phase AC systems☆

Robert Griñó [a,*], Romeo Ortega [b,c], Emilia Fridman [d], Jin Zhang [d], Frédéric Mazenc [e]

[a] Institute of Industrial and Control Engineering, Universitat Politècnica de Catalunya, Diagonal 647, 08028 Barcelona, Spain
[b] ITAM, Campus Río Hondo, Río Hondo #1, 01080 Ciudad de México, Mexico
[c] Adaptive and Nonlinear Control Systems Lab, ITMO University, Kronverksky av., 49, 197101 Saint Petersburg, Russia
[d] Department of Electrical Engineering and Systems, Tel Aviv University, 6997801 Tel Aviv, Israel
[e] Inria Saclay, L2S-CNRS-CentraleSupélec, 3 rue Joliot Curie, 91192, Gif-sur-Yvette, France

ARTICLE INFO

Article history:
Received 27 February 2020
Received in revised form 30 March 2021
Accepted 14 April 2021
Available online xxxx

Keywords:
AC electrical networks
Constant power load
Behavioural model
Stability
Delay-differential equations

ABSTRACT

Constant power loads (CPLs) in power systems have a destabilizing effect that gives rise to significant oscillations or to network collapse, motivating the development of new methods to analyse their effect in AC and DC power systems. A *sine qua non* condition for this analysis is the availability of a suitable mathematical model for the CPL. In the case of DC systems power is simply the product of voltage and current, hence a CPL corresponds to a first–third quadrant hyperbola in the loads voltage–current plane. The same approach is applicable for balanced three-phase systems that, after a rotation of the coordinates to the synchronous frame, can be treated as a DC system. Modelling CPLs for single-phase (or unbalanced poly-phase) AC systems, on the other hand, is a largely unexplored area because in AC systems (active and reactive) power involves the integration in a finite window of the product of the voltage and current signals. In this paper we propose a simple dynamic model of a CPL that is suitable for the analysis of single-phase AC systems. We give conditions on the tuning gains of the model that guarantee the CPL behaviour is effectively captured.

1. Introduction

In many electric power distribution systems and particularly in microgrids, stability problems may occur when a major proportion of the loads are electronic equipment. This kind of equipment is usually powered by cascade distributed architectures which are characterized by the presence of different voltage levels and power electronic converters. These converters act as interfaces between sections of different voltages in which, at last stage, loads are a combination of power electronic converters tightly regulating their output voltage, behaving as Constant Power Loads (CPLs). These architectures are common in information and communication technology facilities where the many telecom switches, wireless communication base stations, and data centre servers act as CPLs. It is well-known that CPLs introduce a destabilizing effect that gives rise to significant oscillations or even voltage collapse, and hence they are considered to be the most challenging component of the standard load model—referred to as the ZIP model in power system stability analysis. See Karimipour and Salmasi (2015), Machado (2019), Molinas, Moltoni, Fascendini, Suul, and Undeland (2008) and Singh, Gautam, and Fulwani (2017) for a recent review of the literature and Matveev, Machado, Ortega, Schiffer, and Pyrkin (2020) for a detailed analysis of the effect of CPLs on the power systems behaviour.

The growing presence of CPLs in modern installations significantly aggravates this issue, hence motivating the development of new methods to analyse their effect in AC and DC power systems. To carry out this analysis it is necessary to dispose a mathematical model that suitably describes the behaviour of the CPL. In the case of a DC system a suitable model for the CPL is simply a first–third quadrant hyperbola in the loads voltage–current plane, $i(t) = \frac{P}{v(t)}$, and, consequently, the load incrementally behaves as a negative resistance contributing to reduce the relative stability of the

☆ The work of Robert Griñó was supported in part by the Government of Spain through the *Agencia Estatal de Investigación*, Spain Project DPI2017-85404-P and in part by the *Generalitat de Catalunya*, Spain under Project 2017 SGR 872. The work of Emilia Fridman and Jin Zhang was supported by Israel Science Foundation (grant no. 673/19) and by the Planning and Budgeting Committee Fellowship from the Council for Higher Education, Israel. The material in this paper was not presented at any conference. This paper was recommended for publication in revised form by Associate Editor Antonella Ferrara under the direction of Editor Thomas Parisini.

* Corresponding author.
E-mail addresses: roberto.grino@upc.edu (R. Griñó), romeo.ortega@itam.mx (R. Ortega), emilia@tauex.tau.ac.il (E. Fridman), zhangjin1116@126.com (J. Zhang), frederic.mazenc@l2s.centralesupelec.fr (F. Mazenc).

https://doi.org/10.1016/j.automatica.2021.109744
0005-1098/

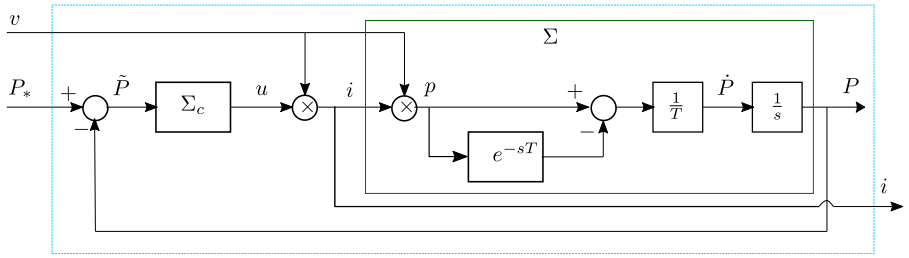

Fig. 1. Block diagram representation of the system (6) in closed-loop with feedback controller Σ_c. The light blue box encloses all the CPL device with port voltage and desired active power inputs and current output. (For interpretation of the references to colour in this figure legend, the reader is referred to the web version of this article.)

electrical network and even to destabilize it (Marx, Magne, Nahid-Mobarakeh, Pierfederici, & Davat, 2012; Riccobono & Santi, 2014). The same model is applicable for balanced three-phase systems that, after a rotation of the coordinates to the synchronous frame, can be treated as a DC system. Modelling CPLs for single-phase (or unbalanced multi-phase) AC systems, on the other hand, is a largely unexplored area because of the definition of active power ($P(t)$) in AC systems (Garcia-Canseco, Griñó, Ortega, Salichs, & Stankovic, 2007; IEEE, 2010), which involves the integration in a finite moving window of the product of the voltage and current signals, more precisely, for a single-phase AC system[1] we have

$$P(t) = \frac{1}{T}\int_{t-T}^{t} v(s)i(s)ds, \tag{1}$$

where $v(t)$ is the voltage and $i(t)$ the current. Throughout the paper we make the following assumption.

Assumption 1. The voltage $v(t)$ is T-periodic, *i.e.*, $v(t) = v(t+T)$, for all $t \geq 0$.

In this paper we propose a simple dynamic model of a CPL that is suitable for the analysis of single-phase AC systems.[2] Because of space limitations we have concentrated in the emulation of active power. However, the extension to include reactive power is immediate and is explained in Section 6. To derive the model we adopt a control theory perspective and reformulate the problem as the design of a negative feedback controller wrapped around the output of a dynamical system that computes $P(t)$. The voltage, required in the computation of $P(t)$, is viewed as an external periodic signal. The control objectives are to drive $P(t)$ to some constant desired value and to ensure that the current is in phase with the voltage. In spite of the apparent simplicity of the aforementioned control problem, it is a far from trivial task because the dynamics of the power computation model is a (T-periodic) linear time-varying delay-differential equation (LTV-DDE), complicating the design of the required controller.

We consider in the paper two controllers: a simple proportional one with a constant bias input and a classical proportional–integral (PI) controller. A detailed analysis of the stability of the closed-loop is carried out using advanced techniques of delay-differential systems. Thus, the stability analysis under PI controller employs a recent time-delay approach to averaging (Fridman & Zhang, 2020). The outcome of this study is the definition of regions in the space of the controller parameters for which asymptotic stability is ensured. To check how conservative the bounds derived from the theoretical analysis are, we carry out extensive numerical simulations and the computation of the more relevant characteristic multipliers of the linear periodic DDEs that arise.

To the best of the authors' knowledge this is the first attempt to develop a mathematically well-founded model for AC CPL's. Most of the results been restricted to numerical derivations (Dong, Liu, Gao, & Zhang, 2008) or invoking various kinds of approximations to the actual phenomenon (Molinas et al., 2008).

2. Problem formulation

In this section we describe the dynamical system that computes the active power $P(t)$ defined in (1) as an LTV operator $\Sigma : (v, i) \mapsto P$. From (1) we get the DDE satisfied by $P(t)$ as

$$\dot{P}(t) = \frac{1}{T}[p(t) - p(t-T)]. \tag{2}$$

where, for ease of reference, we have defined the instantaneous active power

$$p(t) = v(t)i(t). \tag{3}$$

A block diagram description of the system Σ is given in the green box of Fig. 1, where $v(t)$ is a fixed T-periodic, external signal and $i(t)$ as the "control" to be defined. As explained in the introduction, to derive our dynamic model of the AC CPL we adopt a control theory perspective. To generate the input signal $i(t)$ of the system Σ we propose a classical output feedback configuration with $\Sigma_c : \tilde{P} \mapsto u$ the controller to be defined, and $\tilde{P}(t) := P_\star - P(t)$, with $P_\star$ the desired value for $P(t)$. To capture our objective of ensuring that, in steady-state, the voltage and the current are in phase, we define the latter as

$$i(t) = u(t)v(t). \tag{4}$$

In this case, the "in-phase" requirement translates to the condition that $u(t)$ converges to a constant value. A block diagram description of the overall system is given in Fig. 1.

To complete the description of the mathematical model of the system Σ, we note that from (3) and (4) we have $p(t) = v^2(t)u(t)$. Then (1) can be rewritten as

$$P(t) = \frac{1}{T}\int_{t-T}^{t} v^2(\ell)u(\ell)d\ell, \tag{5}$$

revealing that $P(t)$ is just an average of $v^2(t)u(t)$. Differentiating the latter equation, we arrive at the final description of our system

$$\dot{P}(t) = \frac{v^2(t)}{T}[u(t) - u(t-T)]. \tag{6}$$

We are now in position to formulate our controller design problem.

Control problem formulation Consider the LTV, delay-differential, periodic, scalar system (6). Given $P_\star > 0$, design a

[1] It is worth to remark that this definition computes the active power (W) for sinusoidal and nonsinusoidal (general T-periodic) AC single-phase systems and it is the causal version of the expression that appears in IEEE (2010).

[2] For AC poly-phase systems definition (1) changes to $P(t) = \frac{1}{T}\int_{t-T}^{t} \mathbf{v}^\top(s)\mathbf{i}(s)ds$ where $\mathbf{v}(t)$ and $\mathbf{i}(t)$ are, for example, the line-to-neutral voltages vector and the line currents vector, respectively.

controller $\Sigma_c : \tilde{P} \to u$ such that

$$\lim_{t\to\infty} P(t) = P_\star$$
$$\lim_{t\to\infty} u(t) = u_\star \tag{7}$$

where $u_\star > 0$ is an arbitrary constant.

In the following two sections we will present two controllers Σ_c: a simple proportional one with a constant bias input and a classical proportional–integral (PI) controller. For both schemes, we give conditions on their tuning gains that ensure the control objective (7) is satisfied with all signals remaining bounded.

Remark 1. A particular case of practical interest is

$$v(t) = \sqrt{2}\, V \sin\left(\tfrac{2\pi}{T} t\right) \tag{8}$$

where $V > 0$ is the RMS value of the voltage $v(t)$ defined as

$$V^2 := \tfrac{1}{T}\int_0^T v^2(\ell) d\ell. \tag{9}$$

3. A simple proportional plus constant bias controller

The main result of this section is given in the proposition below whose proof, to enhance readability, is given in Appendix A.

Proposition 1. *Consider the simple proportional plus constant bias control law*

$$u(t) = k_p \tilde{P}(t) + u_\star \tag{10}$$

with $u_\star = \frac{1}{V^2} P_\star$ and V the RMS value of the voltage $v(t)$ given by (9), which satisfies Assumption 1. For all values of k_p in the interval $\left(0, \frac{1}{V}\right)$ the conditions (7) are satisfied—with the convergence being exponential. □

Remark 2. It is shown in the proof that, when $P_\star$ is fixed, the $u_\star$ given in Proposition 1 is the unique value that can be obtained for the limit of $u(t)$ if both $P(t)$ and $u(t)$ converge to constant values. From the proof it also follows that $\frac{\ln k_p V}{T}$ is an upperbound on the exponential rate of convergence.

Remark 3. As it is well-known, to enhance the robustness of the system, it is necessary to implement feedback – as opposed to open-loop – control laws. In any case, it is of mathematical interest to observe from (A.1) that setting $k_p = 0$, that is, considering the feedforward controller $u = u_\star$, convergence of the error to zero is achieved in finite time. Actually, it is also possible to show that convergence is preserved even for negative values of k_p in the interval $\left(-\frac{1}{V}, \frac{1}{V}\right)$ and that the trajectories of the closed-loop system remain *bounded* for all k_p. Since the analysis is quite involved, and the boundedness property not very informative, it is omitted for brevity.

4. A proportional–integral controller

In this section we analyse the behaviour of the closed-loop system when Σ_c is a PI controller. That is,

$$\dot{x}_c(t) = \tilde{P}(t)$$
$$u(t) = k_p \tilde{P}(t) + k_i x_c(t) \tag{11}$$

with $k_p \geq 0$ and $k_i > 0$. As in the previous controller our objective is to find conditions on (k_p, k_i)—given in terms of feasibility of linear matrix inequalities (LMIs)—such that the control objective (7) is satisfied. We consider two possible scenarios, when $v^2(t)$ is T-periodic, or $\frac{T}{2}$-periodic. The motivation to consider the two cases is two-fold: on one hand, the LMIs are less conservative when considering smaller periods. On the other hand, the case of practical interest (8) is,[3] indeed, $\frac{T}{2}$-periodic.

The proposition below, whose proof is given in Appendix B, pertains to the T-periodic case.

Proposition 2. *Let $v^2(t)$ be T-periodic.*
(i) Consider the PI controller given by (11) with $k_p > 0$ and $k_i > 0$. Given $k_p^M > 0$ and $k_i^M > 0$, if there exist scalars $r > 0$, $r_1 > 0$, $s > 0$ and $q > 0$ such that the following LMIs are satisfied

$$\Xi_0 = -s + 2v_M^4[(k_p^M)^2 s + (k_i^M)^2(r+q)] + \tfrac{1}{T^2} r_1 < 0, \tag{12}$$

and

$$\Xi(k_p^M, k_i^M) = \begin{bmatrix} \Xi_{11}(k_p^M, k_i^M) & V^2 & 1 & 1 \\ * & -\frac{4}{T} r & -1 & -1 \\ * & * & -\frac{1}{v_M^4 T} q & 0 \\ * & * & * & -\frac{1}{v_M^4 T} r_1 \end{bmatrix} < 0, \tag{13}$$

where we defined the function

$$\Xi_{11}(k_p^M, k_i^M) := -2V^2 + 2v_M^4 T[(k_p^M)^2 s + (k_i^M)^2(r+q)],$$

and

$$v_M := \max_{t\in[0,T]} v(t), \tag{14}$$

then (7) is satisfied for all $k_p \in [-k_p^M, k_p^M]$ and $k_i \in (0, k_i^M]$.
(ii) Consider the I controller given by (11) with $k_p = 0$ and $k_i > 0$. Given $k_i^M > 0$, if there exist scalars $r > 0$ and $q > 0$ such that the following LMI

$$\begin{bmatrix} -2V^2 + v_M^4 T (k_i^M)^2 (r+q) & V^2 & 1 \\ * & -\frac{4}{T} r & -1 \\ * & * & -\frac{1}{v_M^4 T} q \end{bmatrix} < 0 \tag{15}$$

holds, then (7) is satisfied for all $k_i \in (0, k_i^M]$. □

As indicated above, if $v^2(t)$ has a smaller fundamental period $\frac{T}{2}$, a less conservative LMI condition may be derived. This result is contained in the corollary below, whose proof is given in Appendix C.

Corollary 1. *Let $v^2(t)$ be $\frac{T}{2}$-periodic.*
(i) Consider the PI controller given by (11) with $k_p > 0$ and $k_i > 0$. Given $k_p^M > 0$ and $k_i^M > 0$, if there exist scalars $r > 0$, $r_1 > 0$, $s > 0$ and $q > 0$ such that the following LMIs are satisfied

$$\hat{\Xi}_0 = -s + 2v_M^4[(k_p^M)^2 s + (k_i^M)^2(\tfrac{r}{2}+q)] + \tfrac{1}{T^2} r_1 < 0, \tag{16}$$

and

$$\hat{\Xi}(k_p^M, k_i^M) = \begin{bmatrix} \hat{\Xi}_{11}(k_p^M, k_i^M) & V^2 & 1 & 1 \\ * & -\frac{8}{T} r & -1 & -1 \\ * & * & -\frac{16}{9 v_M^4 T} q & 0 \\ * & * & * & -\frac{1}{v_M^4 T} r_1 \end{bmatrix} < 0, \tag{17}$$

where we defined the function

$$\hat{\Xi}_{11}(k_p^M, k_i^M) := -2V^2 + 2v_M^4 T[(k_p^M)^2 s + (k_i^M)^2(\tfrac{r}{2}+q)],$$

and v_M is given by (14), then (7) is satisfied for all $k_p \in [-k_p^M, k_p^M]$ and $k_i \in (0, k_i^M]$.
(ii) Consider the I controller given by (11) with $k_p = 0$ and $k_i > 0$. Given $k_i^M > 0$, if there exist scalars $r > 0$ and $q > 0$ such that the following LMI

$$\begin{bmatrix} -2V^2 + v_M^4 T (k_i^M)^2 (\frac{r}{2}+q) & V^2 & 1 \\ * & -\frac{8}{T} r & -1 \\ * & * & -\frac{16}{9 v_M^4 T} q \end{bmatrix} < 0 \tag{18}$$

holds, then (7) is satisfied for all $k_i \in (0, k_i^M]$. □

[3] Another real case of interest is when $v(t)$ is a T-periodic signal with only odd harmonics (with zero average). In this situation $v^2(t)$ is also a $\frac{T}{2}$-periodic signal.

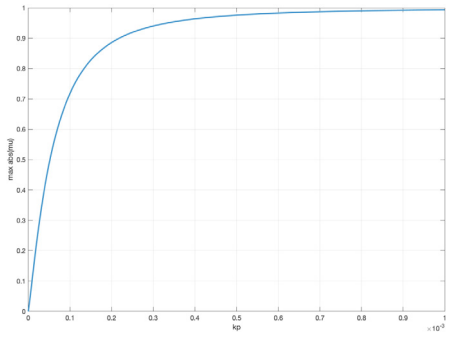

Fig. 2. Maximum absolute value characteristic multiplier vs. k_p.

Remark 4. As it is seen from LMIs of Proposition 2 and Corollary 1, given $T > 0$, these LMIs hold with $k_p^M = k_i^M = 0$. Thus, these LMIs hold for sufficiently small PI gains, i.e. (7) is always guaranteed for small enough $k_p \geq 0$ and $k_i > 0$.

Remark 5. The claim that LMIs (16) and (17) are less conservative than the LMIs (12) and (13) can be established noting that $\hat{\Xi}_0 - \Xi_0 \leq 0$ and $\hat{\Xi}(\cdot) - \Xi(\cdot) \leq 0$ hold. Note also that LMI (13) with $k_p = 0$ is more conservative than LMI (15) in Proposition 2 because its 11-term $-2V^2 + 2v_M^4 T(k_i^M)^2(r+q)$ is larger than 11-term $-2V^2 + v_M^4 T(k_i^M)^2(r+q)$ in (15). The same holds for LMIs (17) and (18) in Corollary 1.

5. Numerical simulation results

This section shows some simulation results and numerical stability assessment, using the characteristic multipliers of the monodromy matrix of the closed-loop delay-differential system, for the AC sinusoidal voltage (8) with $V = 230.0$ V, $T = 0.02$ s. The computation of the characteristic multipliers has been done with the algorithm `eigTMN` (Breda, Maset, & Vermiglio, 2015).

Remark 6. The proposed behavioural model has been extensively tested numerically against step variations of the RMS value of the grid voltage, V, and there are no stability problems for reasonable variations of that value around the nominal one. Besides, the main theoretical result in Proposition 2 can be extended to a variable in time $V \geq V_0 > 0$ that takes values in the given interval. This extension is not in the scope of the current paper.

5.1. P controller

Using the controller in Eq. (10), the closed-loop dynamics is

$$\dot{P}(t) = \frac{-k_p}{T} v^2(t) P(t) + \frac{k_p}{T} v^2(t) P(t-T) \tag{19}$$

and the sufficient condition in Proposition 1 states that it would be stable for $k_p \in \left(0, \frac{1}{V}\right) = \left(0, 4.348 \cdot 10^{-3}\right)$.

The numerical study of the stability of Eq. (19) is shown in Fig. 2 where the maximum absolute value characteristic multiplier is plotted against k_p. As it can be observed, the closed-loop system is *stable for all positive values* of k_p—revealing that, at least for this particular numerical scenario, the theoretical analysis is very conservative. As it can be seen from the figure, the closed-loop system tends to be marginally stable as $k_p \to \infty$.

Fig. 3 shows the power, $P(t)$, and the control signal, $u(t)$, time responses for a step reference in power, $P_\star = 1000$ W, for three different values of k_p. As it can be observed, the steady-state error is zero and the overshoot in the transient increases as k_p gets bigger. In Fig. 4 we plot the voltage applied to the CPL and the computed current for the same three different values of k_p. After the transient, with bigger overshoot as k_p grows, the current is sinusoidal and perfectly in-phase with the voltage.

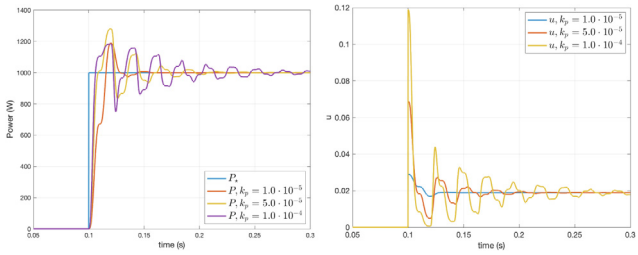

Fig. 3. $P_\star$ and $P(t)$ (left), and $u(t)$ (right) for the proportional controller.

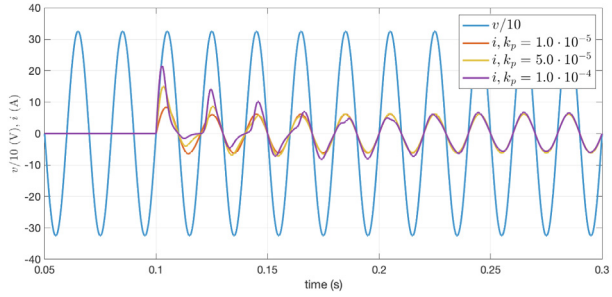

Fig. 4. Voltage, $v(t)/10$, and CPL current $i(t)$ for the proportional controller.

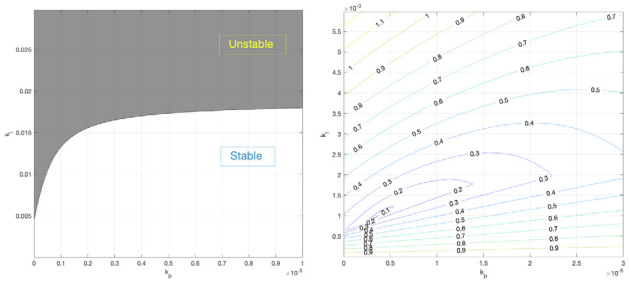

Fig. 5. (k_p, k_i) stability charts: (left) stability regions and (right) contour lines for the maximum absolute value characteristic multiplier near $k_p = 0$ and $k_i = 0$.

5.2. PI controller

In this subsection we investigate *numerically* the PI controller (11) with $k_p > 0, k_i > 0$, which results in the closed-loop dynamics

$$\begin{bmatrix} \dot{\tilde{P}}(t) \\ \dot{x}_c(t) \end{bmatrix} = \begin{bmatrix} \frac{-k_p}{T} v^2(t) & \frac{-k_i}{T} v^2(t) \\ 1 & 0 \end{bmatrix} \begin{bmatrix} \tilde{P}(t) \\ x_c(t) \end{bmatrix} + \begin{bmatrix} \frac{k_p}{T} v^2(t) & \frac{k_i}{T} v^2(t) \\ 0 & 0 \end{bmatrix} \begin{bmatrix} \tilde{P}(t-T) \\ x_c(t-T) \end{bmatrix}. \tag{20}$$

Fig. 5 (left) shows the stability chart in the parameter plane (k_p, k_i), where the shaded area in solid grey corresponds to unstable behaviour. This information has been obtained looking for the maximum absolute value characteristic multiplier of a rectangular sampling of the parameter space k_p - k_i. In Fig. 5 (right) we show the contour lines for the maximum absolute value characteristic multiplier in the plane (k_p, k_i) for k_p and k_i close to zero. It is worth to mention that in the other three quadrants of the plane $k_p - k_i$ the system is unstable.

Looking for the k_p and k_i values that give the minimum maximum absolute value characteristic multiplier ($\min_{k_p, k_i}$

Table 1
Maximum value of k_i^M for different k_p^M via LMIs of Proposition 2 and Corollary 1.

k_p^M	0	$1 \cdot 10^{-6}$	$2 \cdot 10^{-6}$	$4 \cdot 10^{-6}$	$6 \cdot 10^{-6}$
Proposition 2	$2.2923 \cdot 10^{-4}$	$1.6027 \cdot 10^{-4}$	$1.5466 \cdot 10^{-4}$	$1.2985 \cdot 10^{-4}$	$0.7140 \cdot 10^{-4}$
Corollary 1	$3.1077 \cdot 10^{-4}$	$2.1727 \cdot 10^{-4}$	$2.0967 \cdot 10^{-4}$	$1.7604 \cdot 10^{-4}$	$0.9680 \cdot 10^{-4}$

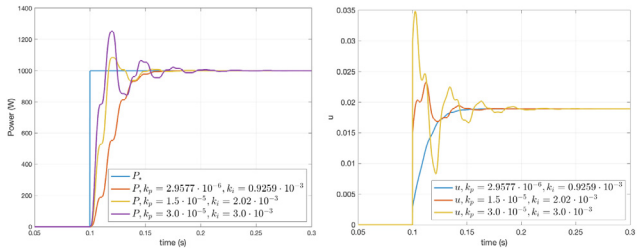

Fig. 6. $P_\star$ and $P(t)$ (left) and $u(t)$ (right) for the PI controller.

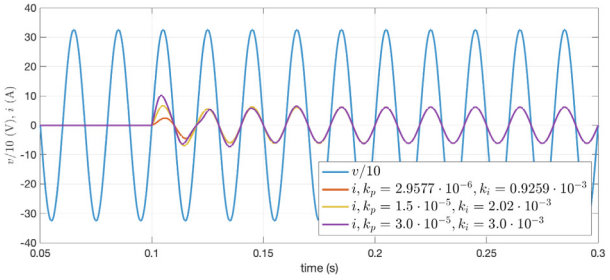

Fig. 7. Voltage, $v(t)/10$ and CPL current $i(t)$ for the PI controller.

$\max_l |\mu_l(k_p, k_i)|$) results[4] in $k_p = 2.95767 \cdot 10^{-6}$, $k_i = 0.92594 \cdot 10^{-3}$ with a maximum absolute value characteristic multiplier, $\max_l |\mu_l| = 0.048368$.

Fig. 6 shows responses of the power, $P(t)$, and the control signal, $u(t)$, to a step reference in power, $P_\star = 1000$ W, for different values of k_p and k_i. As it can be observed, the steady-state error is zero due to the integrator included in the controller. The red curve in the left plot and the blue curve in the right plot correspond to the k_p and k_i values of the minimum maximum absolute value characteristic multiplier commented in the previous paragraph. As seen from these plots the resulting transient performance is excellent with no overshoot. In Fig. 7 appears the (scaled) voltage ($v/10$) applied to the CPL and the computed current for the same three different values of k_p and k_i. After the transient, the currents are sinusoidal and perfectly in-phase with the voltage. Table 1 summarizes the numerical LMI results with $v_M = \sqrt{2}\,V$ running the solver with different k_p^M.

6. Concluding remarks and future research

We have presented in the paper a possible scenario for the emulation of CPLs in single-phase AC systems. The inputs of the system are the voltage signal, which is only assumed to be periodic, and the desired value of the constant power load. The in-phase current that will generate this active power is calculated with a dynamic controller. We have tried three different versions of the latter: proportional+bias, integral and proportional+integral, for which we dispose of a rigorous theoretical analysis to determine bounds on their tuning gains, hence these results are compared with numerical validation.

Because of space limitations, we have concentrated in the emulation of active power. However, the extension to include reactive power is immediate. Indeed, reactive power can be calculated[5] as $Q(t) = \frac{-1}{2\pi}\int_{t-T}^{t} \dot{v}(s)i(s)ds$, see Garcia-Canseco et al. (2007) for a control-oriented discussion on reactive power. Taking into account this definition, a single-phase constant reactive power load can be emulated changing, in Fig. 1, the voltage carrier, $v(t)$, by its derivative, $\dot{v}(t)$. Obviously, it is also possible to emulate a constant active and reactive power load using two closed-loop systems: one to compute the current for the constant active power load and the other to compute the current for the constant reactive power load. Then, the total current is the sum of the currents from each system as they are in quadrature.

Appendix A. Proof of Proposition 1

Substituting $u(t) = k_p[P_\star - P(t)] + \frac{1}{V^2}P_\star$ into (5) we obtain

$$P(t) = \tfrac{k_p}{T}\int_{t-T}^{t} v^2(\ell)[P_\star - P(\ell)]d\ell + P_\star, \tag{A.1}$$

or, equivalently,

$$\tilde{P}(t) = -\tfrac{k_p}{T}\int_{t-T}^{t} v^2(\ell)\tilde{P}(\ell)d\ell. \tag{A.2}$$

Consequently, taking into account that the function $v(t)$ is T-periodic, we obtain

$$\begin{aligned}|\tilde{P}(t)| &\le \tfrac{k_p}{T}\int_{t-T}^{t} v^2(\ell)|\tilde{P}(\ell)|d\ell\\ &\le \tfrac{k_p}{T}\int_0^T v^2(\ell)d\ell \sup_{\ell\in[t-T,t]}|\tilde{P}(\ell)|\\ &= k_p V \sup_{\ell\in[t-T,t]}|\tilde{P}(\ell)|, \quad t \ge 0.\end{aligned}$$

By using Lemma 1 in Mazenc, Malisoff, and Niculescu (2017) with the condition $k_p V < 1$, we arrive at $|\tilde{P}(t)| \le \sup_{\ell\in[-T,0]}|\tilde{P}(\ell)|\, e^{\frac{\ln(k_p V)}{T}t}$. Thus, (7) holds. □

Appendix B. Proof of Proposition 2

We will employ Lemma 1 given in Appendix D.

(i) To complete the proof of (i) we make the following simple, but important, observation. For the PI control law (11), we have the relation

$$\begin{aligned}&u(t) - u(t-T) = \int_{t-T}^{t}\dot{u}(\xi)d\xi\\ &= k_p\int_{t-T}^{t}\dot{\tilde{P}}(\xi)d\xi + k_i\int_{t-T}^{t}\tilde{P}(\xi)d\xi.\end{aligned} \tag{B.1}$$

Substituting (B.1) into (6) and taking into account $\dot{\tilde{P}}(t) = -\dot{P}(t)$, we arrive at

$$\dot{\tilde{P}}(t) = -\tfrac{k_p}{T}v^2(t)\int_{t-T}^{t}\dot{\tilde{P}}(\xi)d\xi - \tfrac{k_i}{T}v^2(t)\int_{t-T}^{t}\tilde{P}(\xi)d\xi. \tag{B.2}$$

Then, conditions (7) are satisfied if (B.2) is asymptotically stable.

For the stability analysis of the time-varying system (B.2) with the T-periodic coefficient $v^2(t)$, we suggest to use the averaging method. We will employ a constructive time-delay approach to averaging introduced recently in Fridman and Zhang (2020).

[4] These optimum has been found using several tries of a Nelder–Mead optimization algorithm. So, it cannot be assured that it is the global minimum but it is the best minimum found.

[5] This definition characterizes the reactive power of a load that can be fully compensated using a shunt capacitor or a shunt inductor at its port variables and, for AC sinusoidal systems, single-phase and poly-phase, coincides with the usual equations to compute the reactive power.

Following this approach, we will integrate (B.2) on $t \in [t-T, t]$ for $t \geq T$. Note that similar to Fridman and Shaikhet (2016), we get

$$\frac{1}{T}\int_{t-T}^{t}\dot{\tilde{P}}(\xi)d\xi = \frac{1}{T}[\tilde{P}(t)-\tilde{P}(t-T)] = \frac{d}{dt}[\tilde{P}(t)-G], \tag{B.3}$$

where

$$G = \frac{1}{T}\int_{t-T}^{t}(\xi - t + T)\dot{\tilde{P}}(\xi)d\xi. \tag{B.4}$$

Denote $z(t) := \tilde{P}(t) - G$. Then, integrating (B.2) and taking into account (B.3) we arrive at

$$\begin{aligned}\dot{z}(t) &= -\frac{k_p}{T^2}\int_{t-T}^{t} v^2(\xi)\int_{\xi-T}^{\xi}\dot{\tilde{P}}(\theta)d\theta d\xi \\ &\quad -\frac{k_i}{T^2}\int_{t-T}^{t} v^2(\xi)\int_{\xi-T}^{\xi}\tilde{P}(\theta)d\theta d\xi \\ &= -\frac{k_p}{T^2}\int_{t-T}^{t} v^2(\xi)\int_{\xi-T}^{\xi}\dot{\tilde{P}}(\theta)d\theta d\xi \\ &\quad -\frac{k_i}{T^2}\int_{t-T}^{t} v^2(\xi)\int_{\xi-T}^{\xi} d\theta d\xi\tilde{P}(t) \\ &\quad +\frac{k_i}{T^2}\int_{t-T}^{t} v^2(\xi)\int_{\xi-T}^{\xi}[\tilde{P}(t)-\tilde{P}(\theta)]d\theta d\xi, \quad t \geq T.\end{aligned}$$

The latter equation can be written as

$$\dot{z}(t) = -k_i V^2\tilde{P}(t) + k_i Y + k_i X, \quad t \geq T, \tag{B.5}$$

where

$$\begin{aligned}Y &= \frac{1}{T^2}\int_{t-T}^{t}\int_{\xi-T}^{\xi}\int_{\theta}^{t} v^2(\xi)\dot{\tilde{P}}(\tau)d\tau d\theta d\xi, \\ X &= -\frac{k_p}{k_i T^2}\int_{t-T}^{t}\int_{\xi-T}^{\xi} v^2(\xi)\dot{\tilde{P}}(\theta)d\theta d\xi.\end{aligned} \tag{B.6}$$

Summarizing, if $\tilde{P}(t)$ is a solution to (B.2), then it satisfies the time-delay system (B.5). Therefore, the stability of the time-delay system guarantees the stability of the original system.

We will derive the stability conditions for the time-delay system (B.5) via Lyapunov–Krasovskii's method. Towards this end, we choose the function

$$V_z = z^2(t). \tag{B.7}$$

Differentiating V_z along (B.5) we have

$$\dot{V}_z = 2[\tilde{P}(t)-G][-k_i V^2\tilde{P}(t) + k_i Y + k_i X]. \tag{B.8}$$

By applying Jensen's inequality (D.1), we obtain

$$2G^2 \leq \int_{t-T}^{t}(\xi - t + T)\dot{\tilde{P}}^2(\xi)d\xi, \tag{B.9}$$

whereas via Jensen's inequalities (D.2) and (D.3) we find

$$\begin{aligned}X^2 &= \frac{k_p^2}{k_i^2 T^4}\Big(\int_{t-T}^{t}\int_{\xi-T}^{\xi} v^2(\xi)\dot{\tilde{P}}(\theta)d\theta d\xi\Big)^2 \\ &\leq \frac{k_p^2 v_M^4}{k_i^2 T^4}\Big(\int_{t-T}^{t}\int_{\xi-T}^{\xi}\dot{\tilde{P}}(\theta)d\theta d\xi\Big)^2 \\ &\leq \frac{k_p^2 v_M^4}{k_i^2 T^2}\int_{t-T}^{t}\int_{\xi-T}^{\xi}\dot{\tilde{P}}^2(\theta)d\theta d\xi,\end{aligned} \tag{B.10}$$

$$\begin{aligned}Y^2 &= \frac{1}{T^4}\Big(\int_{t-T}^{t}\int_{\xi-T}^{\xi}\int_{\theta}^{t} v^2(\xi)\dot{\tilde{P}}(\tau)d\tau d\theta d\xi\Big)^2 \\ &\leq \frac{v_M^4}{T^4}\Big(\int_{t-T}^{t}\int_{\xi-T}^{\xi}\int_{\theta}^{t}\dot{\tilde{P}}(\tau)d\tau d\theta d\xi\Big)^2 \\ &\leq \frac{v_M^4}{T}\int_{t-T}^{t}\int_{\xi-T}^{\xi}\int_{\theta}^{t}\dot{\tilde{P}}^2(\tau)d\tau d\theta d\xi\end{aligned} \tag{B.11}$$

with v_M given by (14). To compensate the G-term, similarly to Fridman and Shaikhet (2016), we will use

$$V_G = \frac{k_i}{T} r\int_{t-T}^{t}(\xi - t + T)^2\dot{\tilde{P}}^2(\xi)d\xi, \quad r > 0. \tag{B.12}$$

We have

$$\dot{V}_G = k_i r T^2\dot{\tilde{P}}^2(t) - \frac{2k_i}{T} r\int_{t-T}^{t}(\xi - t + T)\dot{\tilde{P}}^2(\xi)d\xi. \tag{B.13}$$

Then, due to (B.9)

$$\dot{V}_G \leq k_i r T^2\dot{\tilde{P}}^2(t) - \frac{4k_i}{T} r G^2. \tag{B.14}$$

For the X-term, we consider

$$V_X = \frac{k_p^2}{k_i T^3} r_1\int_{t-T}^{t}\int_{\xi-T}^{\xi}(\xi - t + T)\dot{\tilde{P}}^2(\theta)d\theta d\xi, \quad r_1 > 0. \tag{B.15}$$

Then,

$$\dot{V}_X = \frac{k_p^2}{k_i T^3} r_1\Big(T\int_{t-T}^{t}\dot{\tilde{P}}^2(\xi)d\xi - \int_{t-T}^{t}\int_{\xi-T}^{\xi}\dot{\tilde{P}}^2(\theta)d\theta d\xi\Big). \tag{B.16}$$

Via (B.10), we have

$$\dot{V}_X \leq \frac{k_p^2}{k_i T^2} r_1\int_{t-T}^{t}\dot{\tilde{P}}^2(\xi)d\xi - \frac{k_i}{v_M^4 T} r_1 X^2. \tag{B.17}$$

To compensate the positive term in the right-hand side of (B.17), we employ

$$\tilde{V}_X = \frac{k_p^2}{k_i} s\int_{t-T}^{t}(\xi - t + T)\dot{\tilde{P}}^2(\xi)d\xi, \quad s > 0. \tag{B.18}$$

We have

$$\dot{\tilde{V}}_X = \frac{k_p^2}{k_i} s\Big(T\dot{\tilde{P}}^2(t) - \int_{t-T}^{t}\dot{\tilde{P}}^2(\xi)d\xi\Big). \tag{B.19}$$

From (B.17) and (B.19), it follows that

$$\begin{aligned}\dot{V}_X + \dot{\tilde{V}}_X \leq\ & \frac{k_p^2 T}{k_i} s\dot{\tilde{P}}^2(t) - \frac{k_i}{v_M^4 T} r_1 X^2 \\ & -\frac{k_p^2}{k_i}\Big(s - \frac{1}{T^2} r_1\Big)\int_{t-T}^{t}\dot{\tilde{P}}^2(\xi)d\xi.\end{aligned} \tag{B.20}$$

To compensate Y in (B.8), we consider

$$V_Y = \frac{k_i}{T^2} q\int_{t-T}^{t}\int_{\xi-T}^{\xi}\int_{\theta}^{t}(\xi - t + T)\dot{\tilde{P}}^2(\tau)d\tau d\theta d\xi, \quad q > 0. \tag{B.21}$$

Then,

$$\begin{aligned}\dot{V}_Y &= \frac{k_i}{T} q\int_{t-T}^{t}\int_{\xi-T}^{\xi} d\theta d\xi\cdot\dot{\tilde{P}}^2(t) \\ &\quad +\frac{k_i}{T} q\int_{t-T}^{t}\int_{\theta}^{t}\dot{\tilde{P}}^2(\tau)d\tau d\theta \\ &\quad -\frac{k_i}{T^2} q\int_{t-T}^{t}\int_{\xi-T}^{\xi}\int_{\theta}^{t}\dot{\tilde{P}}^2(\tau)d\tau d\theta d\xi \\ &= \frac{k_i T}{2} q\dot{\tilde{P}}^2(t) + \frac{k_i}{T} q\int_{t-T}^{t}\int_{\theta}^{t}\dot{\tilde{P}}^2(\tau)d\tau d\theta \\ &\quad -\frac{k_i}{T^2} q\int_{t-T}^{t}\int_{\xi-T}^{\xi}\int_{\theta}^{t}\dot{\tilde{P}}^2(\tau)d\tau d\theta d\xi.\end{aligned}$$

Further, by using (B.11) we have

$$\dot{V}_Y \leq \frac{k_i T}{2} q\dot{\tilde{P}}^2(t) + \frac{k_i}{T} q\int_{t-T}^{t}\int_{\theta}^{t}\dot{\tilde{P}}^2(\tau)d\tau d\theta - \frac{k_i}{v_M^4 T} q Y^2. \tag{B.22}$$

To cancel the double integral term in the right-hand side of (B.22), we additionally employ

$$\tilde{V}_Y = \frac{k_i}{T} q\int_{t-T}^{t}\int_{\theta}^{t}(\theta - t + T)\dot{\tilde{P}}^2(\tau)d\tau d\theta. \tag{B.23}$$

Then,

$$\begin{aligned}\dot{\tilde{V}}_Y &= \frac{k_i}{T} q\int_{t-T}^{t}(\theta - t + T)d\theta\dot{\tilde{P}}^2(t) \\ &\quad -\frac{k_i}{T} q\int_{t-T}^{t}\int_{\theta}^{t}\dot{\tilde{P}}^2(\tau)d\tau d\theta \\ &= \frac{k_i T}{2} q\dot{\tilde{P}}^2(t) - \frac{k_i}{T} q\int_{t-T}^{t}\int_{\theta}^{t}\dot{\tilde{P}}^2(\tau)d\tau d\theta.\end{aligned} \tag{B.24}$$

From (B.14), (B.20), (B.22) and (B.24), we obtain

$$\begin{aligned}&\dot{V}_G + \dot{V}_X + \dot{\tilde{V}}_X + \dot{V}_Y + \dot{\tilde{V}}_Y \\ &\leq k_i T(r + q + \frac{k_p^2}{k_i^2} s)\dot{\tilde{P}}^2(t) - \frac{4k_i}{T} r G^2 - \frac{k_i}{v_M^4 T} r_1 X^2 \\ &\quad -\frac{k_i}{v_M^4 T} q Y^2 - \frac{k_p^2}{k_i}\Big(s - \frac{1}{T^2} r_1\Big)\int_{t-T}^{t}\dot{\tilde{P}}^2(\xi)d\xi.\end{aligned} \tag{B.25}$$

Employing (B.2) and further using Young's inequality and Jensen's inequality (3.87) in Fridman (2014) we have

$$\begin{aligned}\dot{\tilde{P}}^2(t) &\leq \frac{v_M^4}{T^2}[k_p\int_{t-T}^{t}\dot{\tilde{P}}(\xi)d\xi + k_i\int_{t-T}^{t}\tilde{P}(\xi)d\xi]^2 \\ &\leq \frac{2v_M^4}{T^2}[k_p^2(\int_{t-T}^{t}\dot{\tilde{P}}(\xi)d\xi)^2 + k_i^2(\int_{t-T}^{t}\tilde{P}(\xi)d\xi)^2] \\ &\leq \frac{2v_M^4}{T}[k_p^2\int_{t-T}^{t}\dot{\tilde{P}}^2(\xi)d\xi + k_i^2\int_{t-T}^{t}\tilde{P}^2(\xi)d\xi]\end{aligned} \tag{B.26}$$

with v_M given by (14). Substitution of (B.26) into (B.25) leads to the term $2k_i^3 v_M^4(r+q+\frac{k_p^2}{k_i^2}s)\int_{t-T}^t \tilde{P}^2(\xi)d\xi$. To cancel the latter term, we additionally employ

$$V_{v_M} = 2k_i^3 v_M^4(r+q+\tfrac{k_p^2}{k_i^2}s)\textstyle\int_{t-T}^t(\xi-t+T)\tilde{P}^2(\xi)d\xi \tag{B.27}$$

that leads to

$$\dot{V}_{v_M} = 2k_i^3 v_M^4(r+q+\tfrac{k_p^2}{k_i^2}s)(T\tilde{P}^2(t)-\textstyle\int_{t-T}^t \tilde{P}^2(\xi)d\xi). \tag{B.28}$$

Define a Lyapunov functional as

$$\mathcal{V} := V_z + V_G + V_X + \tilde{V}_X + V_Y + \tilde{V}_Y + V_{v_M}, \tag{B.29}$$

where V_z, V_G, V_X, $\tilde{V}_X$, V_Y, $\tilde{V}_Y$ and V_{v_M} are given by (B.7), (B.12), (B.15), (B.18), (B.21), (B.23) and (B.27), respectively. Note that Jensen's inequality (3.87) in Fridman (2014)

$$\textstyle\int_{t-T}^t \phi^2(\xi)d\xi \geq \frac{1}{T}[\int_{t-T}^t \phi(\xi)d\xi]^2$$

with $\phi(s) = (\xi-t+T)\dot{\tilde{P}}(\xi)$ leads to $V_G \geq k_i r G^2$, whereas Jensen's inequality (D.1) leads to $\tilde{V}_X \geq \frac{2k_p^2}{k_i}sG^2$. Hence

$$\begin{aligned}\mathcal{V} &\geq V_z + V_G + \tilde{V}_X \\ &\geq \begin{bmatrix}\tilde{P}(t)\\ G\end{bmatrix}^\top \begin{bmatrix}1 & -1\\ * & 1+k_i r+\frac{2k_p^2}{k_i}s\end{bmatrix}\begin{bmatrix}\tilde{P}(t)\\ G\end{bmatrix} \geq c\tilde{P}^2(t)\end{aligned}$$

with T-independent $c > 0$. Thus, $\mathcal{V}$ is positive definite. Taking into account (B.8), (B.25) and (B.28), via (12), we arrive at

$$\begin{aligned}\dot{\mathcal{V}} &\leq k_i\eta^\top \Xi(k_p,k_i)\eta + \tfrac{k_p^2}{k_i}[-s+2v_M^4(k_i^2(r+q) \\ &\quad +k_p^2 s)+\tfrac{1}{T^2}r_1]\textstyle\int_{t-T}^t \dot{\tilde{P}}^2(\xi)d\xi \\ &\leq k_i\eta^\top \Xi(k_p,k_i)\eta, \quad \eta := \mathrm{col}\{\tilde{P}(t), G, Y, X\},\end{aligned}$$

where $\Xi(\cdot,\cdot)$ is defined by (13). Therefore, conditions (7) are satisfied.

Since k_p and k_i appear only in the positive terms of (12) and $\Xi_{11}(\cdot,\cdot)$, the feasibility of LMIs (12) and (13) with the maximum value of $k_p^M > 0$ and $k_i^M > 0$ implies their feasibility for all $-k_p^M \leq k_p \leq k_p^M$ and $0 < k_i \leq k_i^M$.

(ii) For $k_p^M = 0$, (B.5) holds with $X = 0$, whereas (B.26) is changed by

$$\dot{\tilde{P}}^2(t) \leq \tfrac{k_i^2 v_M^4}{T^2}[\textstyle\int_{t-T}^t \tilde{P}(\xi)d\xi]^2 \leq \tfrac{k_i^2 v_M^4}{T}\textstyle\int_{t-T}^t \tilde{P}^2(\xi)d\xi.$$

Then choosing $\mathcal{V}$ as in (B.29) with $V_X = \tilde{V}_X = 0$ and with V_{v_M} changed by $\frac{1}{2}V_{v_M}$, and using arguments of (i) we arrive at the result. □

Appendix C. Proof of Corollary 1

(i) Averaging of (B.2) over $[t-\frac{T}{2}, t]$ for $t \geq \frac{T}{2}$ leads to (B.5) with

$$\begin{aligned}G &= \tfrac{2}{T}\textstyle\int_{t-\frac{T}{2}}^t(\xi-t+\frac{T}{2})\dot{\tilde{P}}(\xi)d\xi,\\ Y &= \tfrac{2}{T^2}\textstyle\int_{t-\frac{T}{2}}^t\int_{\xi-T}^\xi\int_\theta^t v^2(\xi)\dot{\tilde{P}}(\tau)d\tau d\theta d\xi,\\ X &= -\tfrac{2k_p}{k_i T^2}\textstyle\int_{t-\frac{T}{2}}^t\int_{\xi-T}^\xi v^2(\xi)\dot{\tilde{P}}(\theta)d\theta d\xi.\end{aligned}$$

Then, choosing Lyapunov functional

$$\begin{aligned}\mathcal{V} &= z^2(t) + \tfrac{2k_i}{T}r\textstyle\int_{t-\frac{T}{2}}^t(\xi-t+\frac{T}{2})^2\dot{\tilde{P}}^2(\xi)d\xi \\ &\quad +\tfrac{2k_p^2}{k_i T^3}r_1\textstyle\int_{t-\frac{T}{2}}^t\int_{\xi-T}^\xi(\xi-t+\frac{T}{2})\dot{\tilde{P}}^2(\theta)d\theta d\xi \\ &\quad +\tfrac{k_p^2}{k_i}s\textstyle\int_{t-T}^t(\xi-t+T)\dot{\tilde{P}}^2(\xi)d\xi \\ &\quad +\tfrac{8k_i}{3T^2}q\textstyle\int_{t-\frac{T}{2}}^t\int_{\xi-T}^\xi\int_\theta^t(\xi-t+\frac{T}{2})\dot{\tilde{P}}^2(\tau)d\tau d\theta d\xi \\ &\quad +\tfrac{4k_i}{3T}q\textstyle\int_{t-T}^t\int_\theta^t(\theta-t+T)\dot{\tilde{P}}^2(\tau)d\tau d\theta \\ &\quad +2k_i^3 v_M^4(\tfrac{r}{2}+q+\tfrac{k_p^2}{k_i^2}s)\textstyle\int_{t-T}^t(\xi-t+T)\tilde{P}^2(\xi)d\xi\end{aligned} \tag{C.1}$$

with $r > 0$, $r_1 > 0$, $s > 0$ and $q > 0$, we arrive at

$$\dot{\mathcal{V}} \leq k_i\eta^\top\hat{\Xi}(k_p,k_i)\eta, \quad \eta := \mathrm{col}\{\tilde{P}(t), G, Y, X\},$$

where $\hat{\Xi}(\cdot,\cdot)$ is given by (17).

(ii) The proof of (ii) is similar to (ii) of Proposition 2. □

Appendix D. Jensen's inequalities

Lemma 1. *Denote*

$$\begin{aligned}\mathcal{G} &:= \textstyle\int_a^b f(\xi)x(\xi)d\xi, \quad \mathcal{X} := \int_{t-T}^t\int_{\xi-T}^\xi x(\theta)d\theta d\xi,\\ \mathcal{Y} &:= \textstyle\int_{t-T}^t\int_{\xi-T}^\xi\int_\theta^t x(\tau)d\tau d\theta d\xi,\end{aligned}$$

where $a \leq b$, $f : [a,b] \to \mathbb{R}$, $x(\tau) \in \mathbb{R}^n$ and the integration concerned is well defined. Then, for any $n \times n$ matrix $R > 0$ the following Jensen's inequalities hold:

$$\mathcal{G}^\top R\mathcal{G} \leq \int_a^b |f(\xi)|d\xi\int_a^b |f(\xi)|x^\top(\xi)Rx(\xi)d\xi, \tag{D.1}$$

$$\mathcal{X}^\top R\mathcal{X} \leq T^2\int_{t-T}^t\int_{\xi-T}^\xi x^\top(\theta)Rx(\theta)d\theta d\xi, \tag{D.2}$$

and

$$\mathcal{Y}^\top R\mathcal{Y} \leq T^3\int_{t-T}^t\int_{\xi-T}^\xi\int_\theta^t x^\top(\tau)Rx(\tau)d\tau d\theta d\xi. \tag{D.3}$$

Proof. Inequality (D.1) was proved in Solomon and Fridman (2013). We will prove (D.2) and (D.3). By Schur complement, the following holds

$$\begin{bmatrix}x^\top(\tau)Rx(\tau) & x^\top(\tau)\\ * & R^{-1}\end{bmatrix} \geq 0. \tag{D.4}$$

Integration of (D.4), respectively, from $\xi-T$ to ξ in θ, from $t-T$ to t in ξ, and from θ to t in τ, from $\xi-T$ to ξ in θ, from $t-T$ to t in ξ, where

$$\int_{t-T}^t\int_{\xi-T}^\xi d\theta d\xi = T^2, \quad \int_{t-T}^t\int_{\xi-T}^\xi\int_\theta^t d\tau d\theta d\xi = T^3,$$

and application of Schur complement leads to (D.2) and (D.3). □

References

Breda, D., Maset, S., & Vermiglio, R. (2015). *Stability of linear delay-differential equations - a numerical approach with MATLAB*. Springer.

Dong, Y., Liu, W., Gao, Z., & Zhang, X. (2008). Study of a simulation model of AC constant power load. In *2008 IEEE region 10 conference*.

Fridman, E. (2014). *Introduction to time-delay systems: Analysis and control*. Birkhauser.

Fridman, E., & Shaikhet, L. (2016). Delay-induced stability of vector second-order systems via simple Lyapunov functionals. *Automatica, 74*, 288–296.

Fridman, E., & Zhang, J. (2020). Averaging of linear systems with almost periodic coefficients: A time-delay approach. *Automatica, 122*, Article 109287.

Garcia-Canseco, E., Griñó, R., Ortega, R., Salichs, M., & Stankovic, A. (2007). Power factor compensation of electrical circuits: The nonlinear non-sinusoidal case. *IEEE Control Systems Magazine*, *27*(4), 46–59.

IEEE (2010). *IEEE standard definitions for the measurement of electric power quantities under sinusoidal, nonsinusoidal, balanced, or unbalanced conditions*. IEEE Std 1459-2010.

Karimipour, D., & Salmasi, F. (2015). Stability analysis of AC microgrids with constant power loads based on popov's absolute stability criterion. *IEEE Transactions on Circuits and Systems II: Express Briefs*, *62*(7), 696–700.

Machado, J. (2019). *Some problems on the analysis and control of electrical networks with constant power loads* (Ph.D. thesis), Universite Paris-Saclay.

Marx, D., Magne, P., Nahid-Mobarakeh, B., Pierfederici, S., & Davat, B. (2012). Large signal stability analysis tools in DC power systems with constant power loads and variable power loads—A review. *IEEE Transactions on Power Electronics*, *27*(4), 1773–1787.

Matveev, A. S., Machado, J. E., Ortega, R., Schiffer, J., & Pyrkin, A. (2020). A tool for analysis of existence of equilibria and voltage stability in power systems with constant power loads. *IEEE Transactions on Automatic Control*, *65*(11), 4726–4740.

Mazenc, F., Malisoff, M., & Niculescu, S. (2017). Stability and control design for time-varying systems with time-varying delays using a trajectory-based approach. *SIAM Journal on Control and Optimization*, *55*(1), 533–556.

Molinas, M., Moltoni, D., Fascendini, G., Suul, J., & Undeland, T. (2008). Constant power loads in AC distribution systems: An investigation of stability. In *2008 IEEE international symposium on industrial electronics* (pp. 1531–1536).

Riccobono, A., & Santi, E. (2014). Comprehensive review of stability criteria for DC power distribution systems. *IEEE Transactions on Industry Applications*, *50*(5), 3525–3535.

Singh, S., Gautam, A., & Fulwani, D. (2017). Constant power loads and their effects in DC distributed power systems: A review. *Renewable and Sustainable Energy Reviews*, *72*, 407–421.

Solomon, O., & Fridman, E. (2013). New stability conditions for systems with distributed delays. *Automatica*, *49*(11), 3467–3475.

Robert Griñó received the M.Sc. degree in electrical engineering and the Ph.D. degree in automatic control from the Universitat Politecnica de Catalunya (UPC), Barcelona, Spain, in 1989 and 1997, respectively.

From 1990 to 1991, he was a Research Assistant with the Instituto de Cibernética, UPC. From 1992 to 1998, he was an Assistant Professor with the Automatic Control Department, UPC, where he has been an Associate Professor since 1998. Currently, he is also Director of the Institute of Industrial and Control Engineering (IOC), UPC. His research interests include digital control, nonlinear control, and control of power electronic converters.

Dr. Robert Griñó is a member of the Spanish Committee of Automatica (CEA-IFAC) and an affiliate of the International Federation of Automatic Control (IFAC) and member of its Technical Committee 6.3, "Power and Energy Systems". He is also IEEE Senior Member.

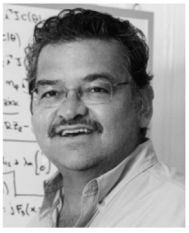

Romeo Ortega was born in Mexico. He obtained his B.Sc. in Electrical and Mechanical Engineering from the National University of Mexico, Master of Engineering from Polytechnical Institute of Leningrad, USSR, and the Docteur D Etat from the Polytechnical Institute of Grenoble, France in 1974, 1978 and 1984 respectively. He then joined the National University of Mexico, where he worked until 1989. He was a Visiting Professor at the University of Illinois in 1987–88 and at McGill University in 1991–1992, and a Fellow of the Japan Society for Promotion of Science in 1990–1991. He was a member of the French National Research Council (CNRS) from June 1992 to July 2020, where he was a "Directeur de Recherche" in the Laboratoire de Signaux et Systemes (CentraleSupelec) in Gif-sur-Yvette, France. Currently, he is a full time Professor at ITAM in Mexico. His research interests are in the fields of nonlinear and adaptive control, with special emphasis on applications. Dr Ortega has published five books and more than 350 scientific papers in international journals, with an h-index of 84. He has supervised more than 35 Ph.D. thesis. He is a Fellow Member of the IEEE since 1999 (Life 2020)and an IFAC Fellow since 2016. He has served as chairman in several IFAC and IEEE committees and participated in various editorial boards of international journals. He is currently Editor in Chief of Int. J. Adaptive Control and Signal Processing and Senior Editor of Asian Journal of Control.

Emilia Fridman received the M.Sc. degree from Kuibyshev State University, USSR, in 1981 and the Ph.D. degree from Voronezh State University, USSR, in 1986, all in mathematics. From 1986 to 1992 she was an Assistant and Associate Professor in the Department of Mathematics at Kuibyshev Institute of Railway Engineers, USSR. Since 1993 she has been at Tel Aviv University, where she is currently Professor of Electrical Engineering-Systems.

She has held visiting positions at the Weierstrass Institute for Applied Analysis and Stochastics in Berlin (Germany), INRIA in Rocquencourt (France), Ecole Centrale de Lille (France), Valenciennes University (France), Leicester University (UK), Kent University (UK), CINVESTAV (Mexico), Zhejiang University (China), St. Petersburg IPM (Russia), Melbourne University (Australia), Supelec (France), KTH (Sweden).

Her research interests include time-delay systems, networked control systems, distributed parameter systems, robust control, singular perturbations and nonlinear control.

She has published more than 190 articles in international scientific journals and two monographs.

She serves/served as Associate Editor in Automatica, SIAM Journal on Control and Optimization and IMA Journal of Mathematical Control and Information. In 2014 she was Nominated as a Highly Cited Researcher by Thomson ISI. Since 2018, she has been the incumbent for Chana and Heinrich Manderman Chair on System Control at Tel Aviv University. She is IEEE Fellow and, currently, a member of the IFAC Council.

Jin Zhang received the Ph.D. degree in control theory and control engineering from Shanghai University, Shanghai, China, in 2018. Since October 2018, he has been a Post-Doctoral Fellow with the School of Electrical Engineering, Tel Aviv University, Tel Aviv, Israel. His research interests include time-delay systems, networked control systems, and event-triggered control.

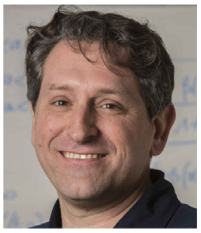

Frédéric Mazenc received his Ph.D. in Automatic Control and Mathematics from the CAS at Ecole des Mines de Paris in 1996. He was a Postdoctoral Fellow at CESAME at the University of Louvain in 1997. From 1998 to 1999, he was a Postdoctoral Fellow at the Centre for Process Systems Engineering at Imperial College. He was a CR from 1999 to 2018. Since 2018, he has been a DR2 at INRIA Saclay. He received a best paper award from the IEEE Transactions on Control Systems Technology at the 2006 IEEE Conference on Decision and Control. His current research interests include nonlinear control theory, differential equations with delay, robust control, and microbial ecology. He has more than 200 peer reviewed publications. Together with Michael Malisoff, he authored a research monograph entitled Constructions of Strict Lyapunov Functions in the Springer Communications and Control Engineering Series.